

Accepted Manuscript

Xanthone Derivatives as Phosphoglycerate Mutase 1 Inhibitors: Design, Synthesis, and Biological Evaluation

Penghui Wang, Lulu Jiang, Yang Cao, Xiaodan Zhang, Bangjing Chen, Shiyu Zhang, Ke Huang, Deyong Ye, Lu Zhou

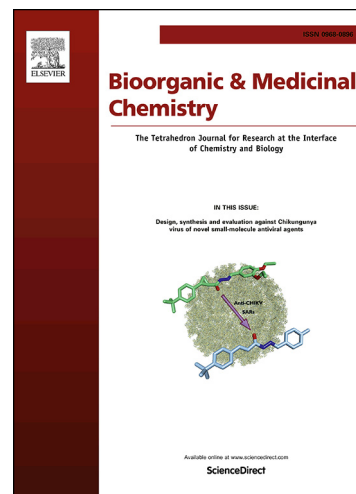
PII: S0968-0896(17)32314-3
DOI: <https://doi.org/10.1016/j.bmc.2018.02.044>
Reference: BMC 14230

To appear in: *Bioorganic & Medicinal Chemistry*

Received Date: 28 November 2017
Revised Date: 17 February 2018
Accepted Date: 23 February 2018

Please cite this article as: Wang, P., Jiang, L., Cao, Y., Zhang, X., Chen, B., Zhang, S., Huang, K., Ye, D., Zhou, L., Xanthone Derivatives as Phosphoglycerate Mutase 1 Inhibitors: Design, Synthesis, and Biological Evaluation, *Bioorganic & Medicinal Chemistry* (2018), doi: <https://doi.org/10.1016/j.bmc.2018.02.044>

This is a PDF file of an unedited manuscript that has been accepted for publication. As a service to our customers we are providing this early version of the manuscript. The manuscript will undergo copyediting, typesetting, and review of the resulting proof before it is published in its final form. Please note that during the production process errors may be discovered which could affect the content, and all legal disclaimers that apply to the journal pertain.



Xanthone Derivatives as Phosphoglycerate Mutase 1 Inhibitors: Design, Synthesis, and Biological Evaluation

Penghui Wang, Lulu Jiang, Yang Cao, Xiaodan Zhang, Bangjing Chen, Shiyu Zhang, Ke Huang, Deyong Ye*, Lu Zhou*

Department of Medicinal Chemistry, School of Pharmacy, Fudan University, No.826, Zhangheng Rd., Shanghai, 201203, China

Abstract

Phosphoglycerate mutase 1 (PGAM1) is a glycolytic enzyme that dynamically converts 3-phosphoglycerate (3PG) to 2-phosphoglycerate (2PG), which was upregulated to coordinate glycolysis, pentose phosphate pathway (PPP) and serine biosynthesis to promote cancer cell proliferation and tumor growth in a variety of cancers. However, only a few inhibitors of PGAM1 have been reported with poor molecular or cellular efficacy. In this paper, a series of xanthone derivatives were discovered as novel PGAM1 inhibitors through scaffold hopping and sulfonamide reversal strategy based on the lead compound PGMI-004A. Most xanthone derivatives showed higher potency against PGAM1 than PGMI-004A and exhibited moderate anti-proliferation activity on different cancer cell lines.

Keywords: Phosphoglycerate mutase 1, Inhibitors, Xanthone derivatives, Cancer cell metabolism

ABBREVIATIONS

PGAM1, Phosphoglycerate mutase 1; 3PG, 3-phosphoglycerate; 2PG, 2-phosphoglycerate; 2,3-BPG, 2,3-bisphosphoglycerate; 6PGD, 6-phosphogluconate dehydrogenase; PPP, pentose phosphate pathway; PHGDH, 3-phosphoglycerate dehydrogenase; SSP, serine synthesis pathway; EGCG, epigallocatechin gallate; SAR, structure activity relationship; IC₅₀, 50% inhibiting concentration

*Corresponding author: Tel. & Fax: +86-21-51980117. E-mail address: dyeye@shmu.edu.cn (D Ye).

*Corresponding author: Tel. & Fax: +86-21-51980125. E-mail address: zhoulu@shmu.edu.cn (L Zhou).

1. Introduction:

Cancer cells tend to competently coordinate bioenergetics, anabolic biosynthesis, and balanced redox status to provide an optimum microenvironment for cancer cell proliferation and tumor growth [1]. This phenotype known as cancer cell metabolic reprogramming has been established as one essential hallmark of cancer cells [2, 3]. The Warburg effect describes a phenomenon that most cancer cells predominantly rely on the high rate of aerobic glycolysis to produce energy rather than efficient mitochondrial oxidative phosphorylation as in most normal cells. The resulting alteration serves to supply the glycolytic intermediates as building blocks for anabolic biosynthesis of macromolecules, such as RNA/DNA, proteins, and lipids and meet the needs of the rapid proliferation of tumor cells [4]. Thus targeting key metabolic enzymes may provide a promising therapeutic strategy for cancer treatment [5-10].

Phosphoglycerate mutase 1 (PGAM1) catalyzes the 8th step of glycolysis, reversibly isomerizing 3-phosphoglycerate (3PG) to 2-phosphoglycerate (2PG) through 2,3-bisphosphoglycerate (2,3-BPG) as a cofactor [11, 12]. In humans, PGAM1 is widely expressed in the non-muscle tissue, such as liver and brain [13]. Meanwhile, it is found to be overexpressed in various types of human cancer, including breast cancer [14], prostate cancer [15], lung cancer [16], oral squamous cell carcinoma [17], hepatocellular carcinoma [18], and urothelial bladder cancer [19]. What's more, both pharmacological inhibition [20-23] and knockdown of PGAM1 result in suppression of cancer cell proliferation, tumor growth [18], and even cancer cell migration [24, 25]. Hitosugi et al. has demonstrated that PGAM1 promotes tumor growth by dynamically regulating the intracellular levels of glycolytic metabolites 3-PG and 2-PG, which function as signaling molecules to directly affect the catalytic activity of 6-phosphogluconate dehydrogenase (6PGD) in the oxidative pentose phosphate pathway (PPP) and 3-phosphoglycerate dehydrogenase (PHGDH) in serine synthesis pathway (SSP) respectively [21]. In addition to upregulated gene expression of PGAM1, oncogenic tyrosine kinases such as FGFR1, EGFR, FLT3 and JAK2 phosphorylate Y26 of PGAM1 enhance its enzymatic activity and promote tumor growth in diverse human cancers [26]. Accordingly, inhibition of PGAM1 can not only reduce the indispensable energy supply for cancer cells but also prevent anabolic processes including PPP and SSP, required for cell proliferation and tumor growth [27]. In summary, developing PGAM1 inhibitors could become a new promising therapeutic opportunity for cancer therapy.

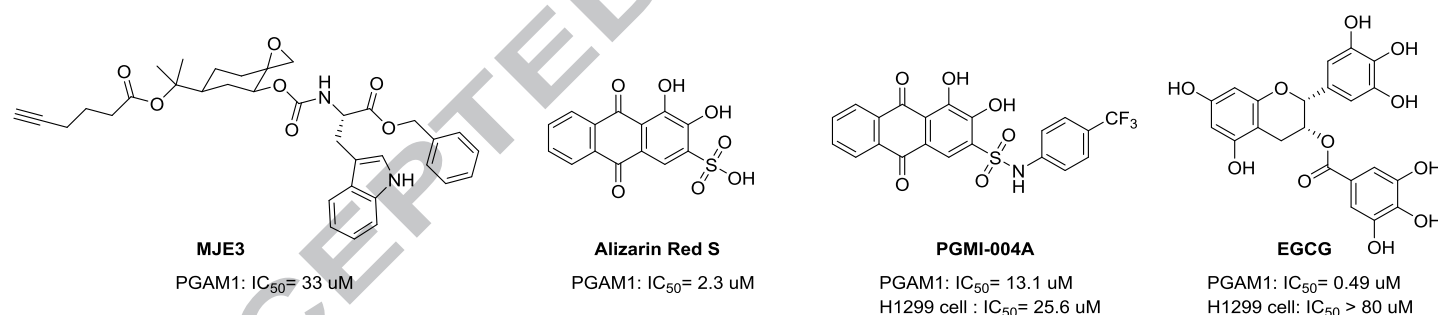


Figure 1 The chemical structures of reported PGAM1 inhibitors.

However, only a small amount of PGAM1 inhibitors with poor cellular efficacy have been reported so far (**Fig. 1**) [20-22]. MJE3 was found to covalently label PGAM1 on K100 by its unique spiroepoxide pharmacophore [28]. Epigallocatechin gallate (EGCG), the major extract from the green tea, was identified as a PGAM1 inhibitor with higher molecular potency but very limited cellular efficacy due to its polyphenol structure [22]. Besides, EGCG could broadly affect multiple signaling pathways [29], suggesting that EGCG had strong off-targets effects. Alizarin Red S (ARS), obtained from high-throughput screening, possessed medium inhibitory activity against PGAM1, while no anti-proliferation activity was shown because of its low permeability caused by the sulfonic acid group. After structure modification of ARS, the sulfonamide PGMI-004A was obtained. PGMI-004A, although with a weak inhibitory activity against PGAM1 *in vitro*, could not only reduce cell proliferation but also suppress tumor growth in xenograft nude mice *in vivo* [21]. Considering the anthraquinone core of PGMI-004A belongs to structural alerts [30] in medicinal chemistry, PGMI-004A is required to be subjected to structural optimization. Herein, we conducted the scaffold hopping to replace the anthraquinone core of PGMI-004A with xanthone core, and take the sulfonamide reversal strategy to design and synthesize a series of xanthone derivatives, which showed stronger efficacy and better specificity than PGMI-004A against PGAM1, as well as higher anti-cell proliferative activity against H1299 cell line. (**Fig. 2**).

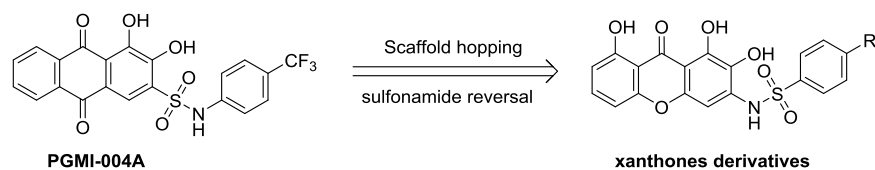
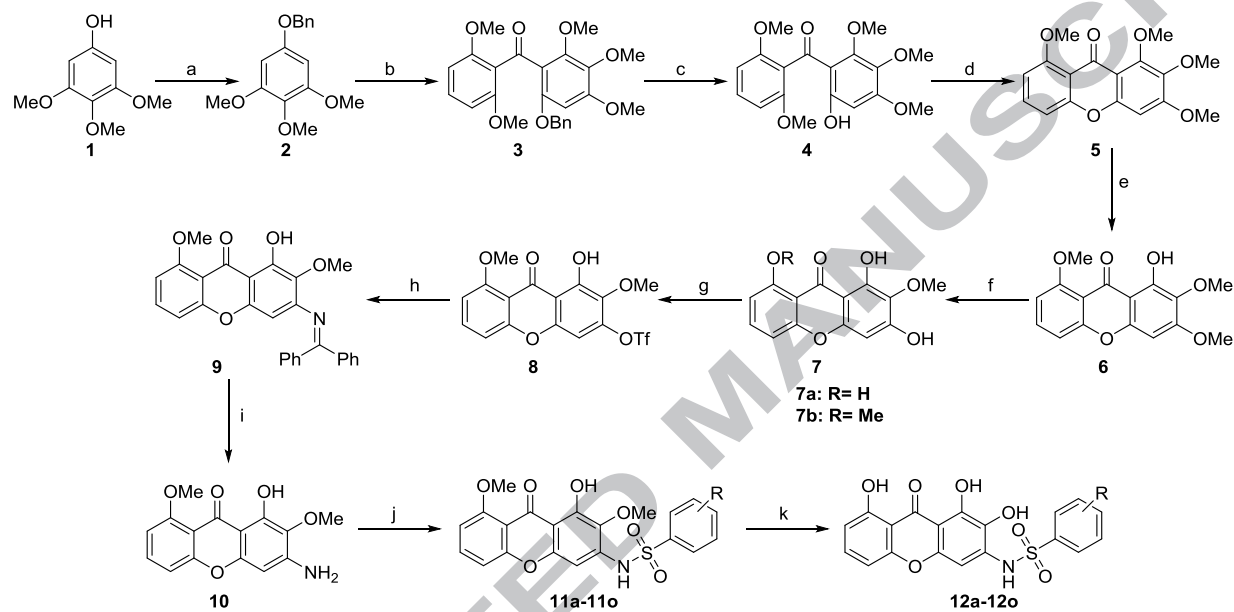


Figure 2 Designing of xanthenes by scaffold hopping and sulfonamide reversal strategy.

2. Results and discussion

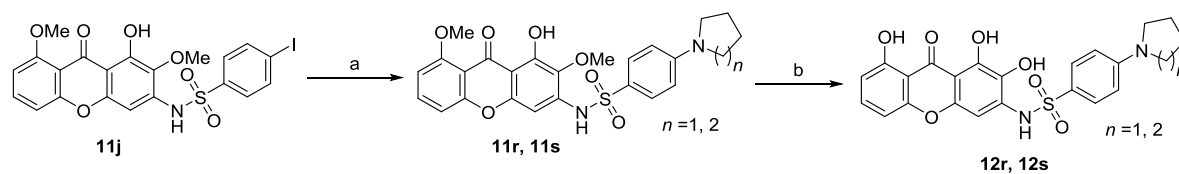
2.1 Chemistry



Scheme 1 General synthetic route of xanthone derivatives. Reagents and conditions: a. BnBr, K_2CO_3 , acetone, r.t., 85%; b. 2,6-dimethoxybenzoic acid, TFAA, DCM, $0^\circ C$, 66%; c. H_2 , Pd/C, THF, r.t., 98%; d. Me_2NOH , pyridine, H_2O , reflux, 92%; e. BCl_3 , DCM, $0^\circ C$, 92%; f. piperidine, H_2O , mw, $120^\circ C$, 50%; g. Tf_2O , pyridine, DCM, $0^\circ C$, 73%; h. $Pd(OAc)_2$, BINAP, diphenylmethanimine, Cs_2CO_3 , dioxane, reflux, 78%; i. HCl, THF, H_2O , r.t., 80%; j. substituted benzenesulfonyl chloride, pyridine, r.t., 40~70%; k. BBr_3 , DCM, $0^\circ C$, 30~50%.

The xanthone derivatives were synthesized as shown in **Scheme 1**. 3,4,5-trimethoxy phenol was protected with benzyl to afford the benzyl ether **2**, which was reacted with dimethoxy benzoic acid via Friedel–Crafts reaction to give benzophenone **3**. After debenzoylation of **3** and cyclization of **4**, the xanthan **5** was obtained and demethylated with 1 eq. boron trichloride to afford the demethylation product **6**. Continued demethylation of compound **6** was achieved via a microwave-assisted modified condition of Gil's work[31] to lead the trihydroxy xanthone **7a** and the dihydroxy xanthone **7b**. **7b** was converted to the triflate **8** by treating with Tf_2O . The key intermediate amino xanthone **10** was obtained via Buchwald–Hartwig amination/hydrolysis protocol [32] from triflate **8**. From the amine **10**, a series of sulfonamides **11** were synthesized and then demethylated the protecting groups with BBr_3 to afford the desired compounds **12a~12p**.

Since the para-*N*-substituted benzenesulfonyl chloride could hardly be separated from its meta isomer during the preparation of 4-(pyrrolidin-1-yl)benzenesulfonyl chloride and 4-(piperidin-1-yl)benzenesulfonyl chloride, as well as the sulfonamide products, **12r** and **12s** were synthesized with an alternative route. The intermediates **11r** and **11s** were synthesized from **11j** with pyrrolidine and piperidine via conventional Buchwald–Hartwig coupling according to **Scheme 2** respectively.

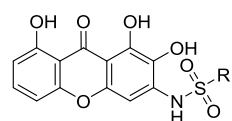


Scheme 2 Synthetic route of 12r and 12s. Reagents and conditions: a. $\text{Pd}_2(\text{dba})_3$, BINAP, *t*-BuONa, pyrrolidine or piperidine, NMP, 100°C; b. BBr_3 , DCM, 0°C, 30~50%.

2.2 Biological evaluation and molecular docking

2.2.1 *In vitro* PGAM1 enzyme inhibitory activity

Table 1. PGAM1 inhibition activity and counter-screen assay of xanthones derivatives



Entry	Compounds	R	PGAM 1 inhibition IC_{50} (μM) ^a	Counter-screen assay ^c (inhibition ratio@ 5 μM)
1	11a-11s		$>> 20 \mu\text{M}$ ^b	ND
2	12a	phenyl	2.8 ± 1.1	6%
3	12b	4-methyl phenyl	7.2 ± 1.8	2%
4	12c	benzyl	1.9 ± 0.4	12%
5	12d	4-(trifluoromethyl)phenyl	3.5 ± 0.8	-1%
6	12e	2,5-bis(trifluoromethyl)phenyl	6.3 ± 1.8	2%
7	12f	3-(trifluoromethoxy)phenyl	5.8 ± 0.4	12%
8	12g	4-fluorophenyl	5.5 ± 2.3	1%
9	12h	4-chlorophenyl	3.6 ± 0.5	15%
10	12i	4-bromophenyl	2.9 ± 0.1	6%
11	12j	4-iodophenyl	1.9 ± 0.2	11%
12	12k	4-cyanophenyl	4.2 ± 0.3	10%
13	12l	3-cyanophenyl	2.1 ± 0.5	13%
14	12m	naphthalen-1-yl	1.7 ± 0.5	7%
15	12n	naphthalen-2-yl	1.6 ± 0.0	9%
16	12o	[1,1'-biphenyl]-4-yl	1.2 ± 0.2	8%
17	12p	4-(<i>tert</i> -butyl)phenyl	2.6 ± 0.4	1%
18	12q	4-cyclohexylphenyl	0.5 ± 0.1	9%
19	12r	4-(pyrrolidin-1-yl)phenyl	2.7 ± 0.1	4%

20	12s	4-(piperidin-1-yl)phenyl	1.0 ± 0.3	5%
21	EGCG		0.49	63% (@0.625 μM)
21	PGMI-004A		13.0 ± 0.1	38%

^aThe IC₅₀ data were presented as mean ± sd. Each experiment was run in triplicate.

^bThe inhibition ratios of **11a-11s** against PGAM1 were less than 10% at 20 μM

^cThe counter-screen assay was conducted to exclude the false-positive results

The enzyme inhibitory activities of the xanthone derivatives were determined by multiple enzymes coupled assay [21]. The results shown in **Table 1** exhibited that all final xanthone products (**12a-12s**) displayed much more potency than PGMI-004A against PGAM1. Especially, **12q** with IC₅₀ of 0.5 μM, compared to PGMI-004A, the PGAM1 inhibitory activity increased by 26 times. Furthermore, the counter-screen assay data were measured to exclude the non-specific inhibitory activity against to PGAM1. EGCG with IC₅₀ of 0.49 μM, showed an inhibition ratio of 63% at a concentration of 0.625 μM in the counter-screen assay system. However, all xanthone derivatives almost showed no inhibitory activities against the latter three downstream enzymes including enolase, pyruvate kinase and lactate dehydrogenase in the multiple enzymes coupled assay system at a concentration up to 5 μM.

In order to explore the interesting enzymatic profiles, a preliminary structure-activity relationship (SAR) was discussed as follow. All final xanthone products (**12a-12s**) showed significant inhibitory activities against PGAM1 as compared to their methylation precursors (**11a-11s**), suggesting that exposed hydroxyl groups in these positions were essential for activities. While for different substituents on the sulfonamide benzene ring, the IC₅₀ values were approximately in the same order of magnitude. This might indicate that the benzene ring binds to a large cave of PGAM1. For the derivatives with mono-substituted on the C4 of the benzene ring, their inhibitory activities were significantly enhanced with the increase of the substituents' volume, such as from **12g** to **12j**, the IC₅₀ values increased from 5.5 μM to 1.9 μM. In addition, the derivatives with a larger ring system (including phenyl, cyclohexyl, heterocycle) substituted on the C4 of benzene ring showed much more potency than those small function group substitutions.

2.2.2 Thermal shift assay

To examine whether **12q** binds to PGAM1, the thermal shift assay was performed to validate the interaction of protein and small molecule (**Fig 3**). Incubation of increasing concentrations from 12.5 μM to 50 μM of **12q** raised PGAM1's melting temperature (T_m) in a dose-dependent manner, suggesting that **12q** directly binds to PGAM1.

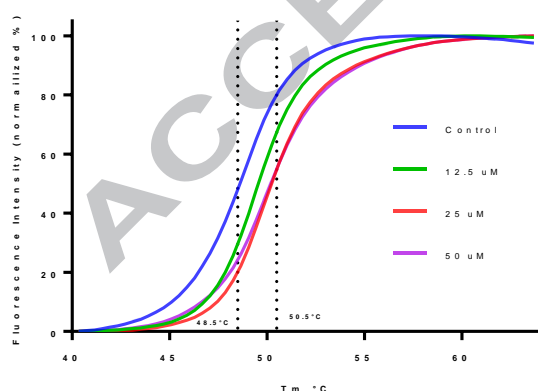


Figure 3 Thermal shift melting curves of PGAM1 and **12q**.

2.2.3 Molecular docking

We selected the representative compounds **12b**, **12q** and **12s** to reveal the structure-activity relationships by using molecular docking. The PGAM1-ARS complex structure model, our unpublished result, showed the ARS bind to the allosteric site next to the substrate-binding

pocket by hydrogen bonds and hydrophobic interaction (**Fig 4A**). Besides, the 1-OH group of ARS was linked with R191 and N209 through a water bridge.

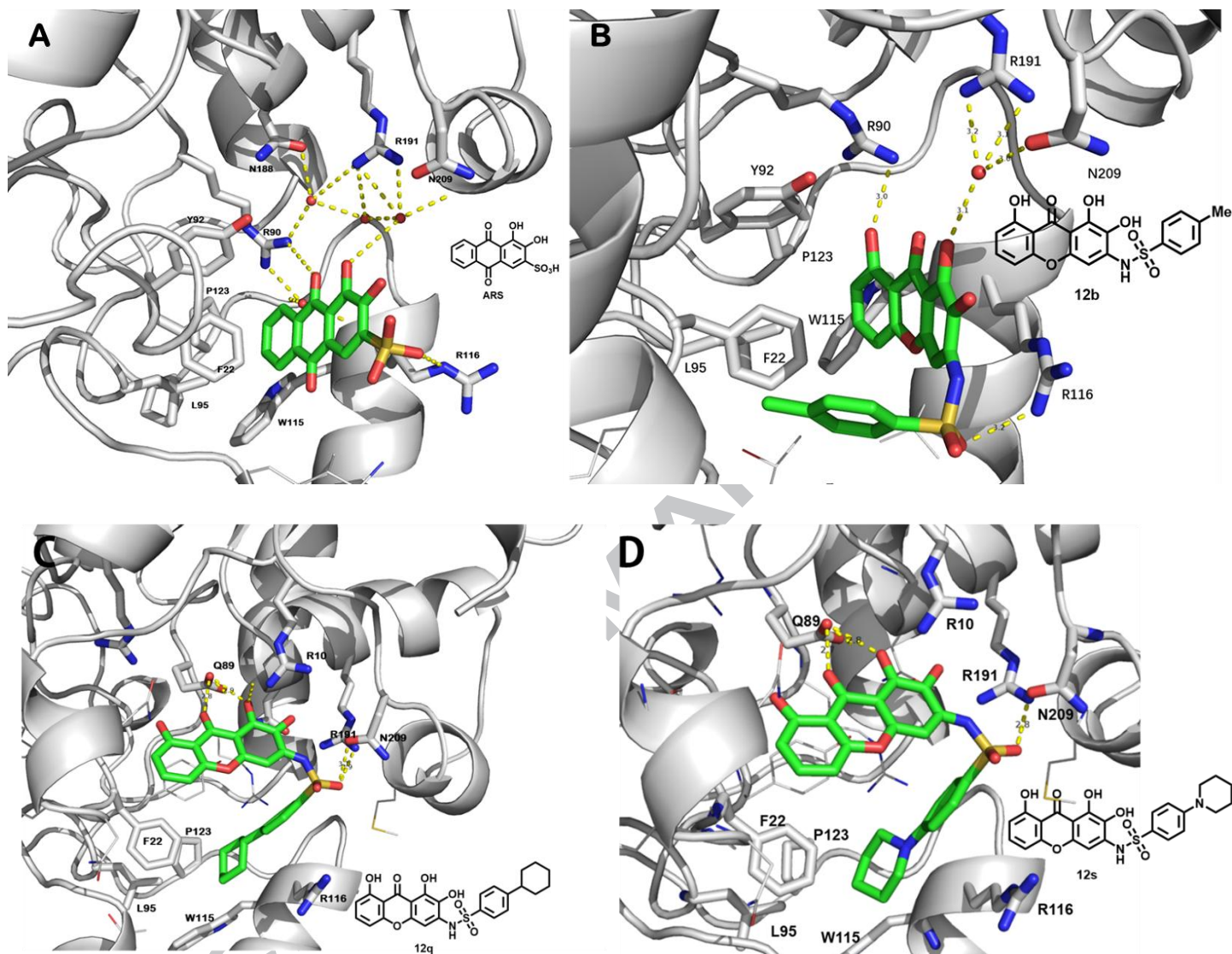
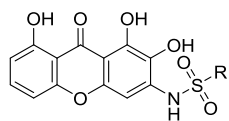


Figure 4 The model of PGAM1- inhibitor interaction (**A**: the crystal structure of the PGAM1-ARS complex; **B**: the docking model of **12b** bind to PGAM1; **C**: the docking model of **12q** bind to PGAM1; **D**: the docking model of **12s** bind to PGAM1)

We retained this water bridge during docking study of compound **12b**. As a result, compound **12b** showed a similar mode of action compare to ARS (**Fig 4B**). The sulfonamide benzene ring formed a weak hydrophobic interaction with F22 in PGAM1. Then the compound **12q** was docked to this model, but no reasonable results generated. We conjectured that the cyclohexyl of **12q** and the piperidin-1-yl of **12s** would result in a spatial collision with F22 in PGAM1 if we take the same docking method with **12b**. Therefore, we abandoned the water bridge during the docking study of compound **12q** and **12s**. The results showed the binding modes of compound **12q** and **12s** with PGAM1 were immensely different with **12b** (**Fig 4C & 4D**). The hydroxyl groups and sulfonamide group contacted with polar residues (including Q89, R191, and N209) through hydrogen bonds directly. Moreover, the cyclohexyl of **12q** and the piperidin-1-yl of **12s** occupied the hydrophobic pocket consisting of P123, W115, and L95, which was held by the xanthone ring in ARS and compound **12b**'s model.

2.2.4 *In vitro* cell proliferation inhibitory activity

Table 2 Anti-proliferation activities of xanthone derivatives

Entry	Compounds	R	H1299	MCF-7	PANC-1
			IC ₅₀ (μM) ^a	IC ₅₀ (μM)	IC ₅₀ (μM)
1	12a	phenyl	59.0 ± 20.6	112.6 ± 38	>200 ^b
2	12b	4-methyl phenyl	13.2 ± 2.0	44.9 ± 1.8	20.7 ± 2.8
3	12c	benzyl	62.9 ± 12.8	>200	>200
4	12d	4-(trifluoromethyl)phenyl	10.3 ± 1.8	30.2 ± 21.4	58.5 ± 17.4
5	12e	2,5-bis(trifluoromethyl)phenyl	16.8 ± 0.8	15.8 ± 3.4	10.5 ± 1.6
6	12f	3-(trifluoromethoxy)phenyl	13.9 ± 0.9	20.5 ± 1.3	116.0 ± 9.8
7	12g	4-fluorophenyl	21.9 ± 2.3	20.8 ± 2.6	>200
8	12h	4-chlorophenyl	10.2 ± 1.1	15.5 ± 5	91.4 ± 5.3
9	12i	4-bromophenyl	> 40 ^c	6.8 ± 3.5	>200
10	12j	4-iodophenyl	24.3 ± 1.9	13.5 ± 2.9	34.5 ± 9.7
11	12k	4-cyanophenyl	> 40	40.1 ± 7.9	>200
12	12l	3-cyanophenyl	53.0 ± 7.8	18.4 ± 4.7	>200
13	12m	naphthalen-1-yl	23.2 ± 0.3	27.3 ± 2.5	100.8 ± 33.7
14	12n	naphthalen-2-yl	22.6 ± 1.2	43.3 ± 12.8	>200
15	12o	[1,1'-biphenyl]-4-yl	12.9 ± 1.2	44.9 ± 1.8	>200
16	12p	4-(<i>tert</i> -butyl)phenyl	10.7 ± 2.5	13.4 ± 3.4	>200
17	12q	4-cyclohexylphenyl	10.7 ± 1.0	26.6 ± 4.0	35.3 ± 4.9
18	12r	4-(pyrrolidin-1-yl)phenyl	5.0 ± 0.9	>200	137.0 ± 11.0
19	12s	4-(piperidin-1-yl)phenyl	8.1 ± 1.5	47.6 ± 16.8	>200
20	PGMI-004A		26.0 ± 2.1	> 40	32.0 ± 3.7

^aThe IC₅₀ data were presented as mean ± sd. Each experiment was run in triplicate.

^bThe inhibition ratios were less than 50% at 200 μM

^cThe inhibition ratios were less than 50% at 40 μM

The MTT cell proliferation assay was employed to evaluate the cell proliferation inhibitory activity of those xanthone derivatives. As mentioned above, PGAM1 was overexpressed in a variety of cancers, such as lung cancer, breast cancer, and pancreatic cancer, so we performed the anti-proliferation assay on the representative cell lines including H1299, MCF-7 and PANC-1 (**Table 2**). For H1299 cells, most of the xanthone derivatives exhibited comparable anti-cell proliferative activity to that of PGMI-004A although the PGAM1 enzymatic inhibitory activities of those xanthone derivatives were significantly stronger than that of PGMI-004A. This might be due to the poor

permeability of the xanthone derivatives. It is worth mentioning that when nitrogen atom was introduced into the saturated ring (**12r** and **12s**) which would increase the solubility, the antiproliferation activities were slightly increased. The most potent compound **12r**'s cellular inhibitory activity (IC_{50} = 5.0 μ M) was increased by 5 times compared to PGMI-004A on H1299 cells. As for MCF-7 and PANC-1 cells, these xanthone derivatives showed weaker inhibition activity. We conjectured the different sensitivity of the above three cell lines to those xanthone derivatives might be caused by the different expression levels of PGAM1.

To validate these xanthone compounds exert anti-proliferative effect through PGAM1, we next measured the anti-proliferation activities of **12e** on PGAM knockdown and overexpressed PANC-1 cells respectively (**Table 3**). The IC_{50} values shifted from 5.1 μ M to 42.8 μ M and 13.8 μ M to 25.0 μ M respectively in PGAM1 knockdown and overexpressed PANC1 cells, suggesting that **12e** exerts anti-proliferative activity by inhibiting PGAM1 at cellular level.

Table 3 Anti-proliferation activities of **12e** on PGAM1 knockdown and overexpressed PANC1 cells

	Blank IC_{50} (μ M) ^a	IC_{50} (μ M)
PGAM1 KD PANC1 cells	5.1 \pm 2.4	42.8 \pm 13.6
PGAM1 overexpressed PANC1 cells	13.8 \pm 4.0	25.0 \pm 5.1

^aThe IC_{50} data were presented as mean \pm sd. Each experiment was run in triplicate

3. Conclusion

In summary, starting from the lead compound PGMI-004A, we discovered a new series of xanthone derivatives as novel PGAM1 inhibitors through scaffold hopping and sulfonamide reversal strategy. Nineteen xanthone sulfonamides were synthesized and biologically evaluated. PGAM1 enzymatic inhibitory activity assays showed that all designed xanthone derivatives exhibited more potency against PGAM1 than PGMI-004A. Especially **12q** with IC_{50} of 0.5 μ M was the most effective PGAM1 specific inhibitor so far which was supported by counter-screen assay and thermal shift assay. Besides, a preliminary SAR of those xanthone derivatives was obtained, and molecular docking revealed the rational binding models of those xanthone derivatives. The anti-proliferation activities of our designed compounds was evaluated on the representative cancer cell lines. What's more, **12e**'s IC_{50} shifts on PGAM1 knockdown and overexpressed PANC-1 cells revealed that **12e** was an effective PGAM1 inhibitor on cellular level.

4. Experimental protocols

Reagents were purchased from commercial suppliers and used without further purification unless specifically noted. Flash column chromatography was carried on CombiFlash® Rf 150 from Teledyne Isco with the standard silica gel column. Mass spectra were given with electrospray ionization (ESI) produced by a Finnigan MAT-95, LCQ-DECA spectrometer and IonSpec 4.7 T. MS. NMR spectra were recorded on a Varian Mercury 400 or 600 spectrometer with tetramethylsilane as an internal reference. OD (Optical density) was measured with a microplate reader (SpectraMax M5, Molecular Devices).

4.1 General procedures for preparation of key intermediate **10**.

4.1.1 5-(benzyloxy)-1,2,3-trimethoxybenzene (**2**).

3,4,5-Trimethoxy phenol (5.0 g, 27.2 mmol) was dissolved in acetone(100 mL), and then K_2CO_3 (5.63 g, 40.7 mmol) was added. After vigorously stirring for 5 min, benzyl bromide (3.4 mL, 28.5 mmol) was added dropwise. The reaction mixture was maintained at room temperature overnight, the solid was filtered out and the reaction solution was concentrated to remove the solvent. The residue was dissolved in ethyl acetate (100 mL) and then washed with 1 mol/L NaOH aqueous solution twice. The organic phase was dried over anhydrous Na_2SO_4 , filtered and concentrated under reduced pressure to afford compound **2** as a white solid (6.36 g, yield: 85%).

4.1.2 (6-(benzyloxy)-2,3,4-trimethoxyphenyl)(2,6-dimethoxyphenyl)methanone (**3**).

The benzyl ether **2** (3.7 g, 13.4 mmol) and 2,6-dimethoxybenzoic acid (2.6 g, 14.1 mmol) were dissolved in dry DCM (140 mL) under an ice-water bath and then 14 mL trifluoroacetic anhydride (TFAA) was added dropwise. After the substrate **2** was disappeared monitoring by TLC, the reaction solution was poured into 150 mL ice-water mixture with vigorously stirring. The organic phase was washed with 1 mol/L NaOH aqueous solution (twice) and brine, dried over anhydrous Na₂SO₄, filtered and concentrated under reduced pressure to afford compound **3** as a white solid (3.93 g, yield: 66%) without purification. ¹H NMR (400 MHz, Chloroform-*d*) δ 7.29 – 7.25 (m, 3H), 7.22 (t, *J* = 8.4 Hz, 1H), 7.16 – 7.12 (m, 2H), 6.48 (s, 1H), 6.46 (s, 1H), 6.26 (s, 1H), 4.89 (s, 2H), 3.83 (s, 3H), 3.80 (s, 3H), 3.73 (s, 3H), 3.57 (s, 6H).

4.1.3 (2,6-dimethoxyphenyl)(6-hydroxy-2,3,4-trimethoxyphenyl)methanone (**4**).

To a solution of ketone **3** (3.93 g, 8.96 mmol) in THF (50 mL) was added 10% Pd/C (100 mg). The reaction mixture was hydrogenated under a hydrogen balloon overnight and then the mixture was filtered through a celite bed, washed with ethyl acetate, and concentrated in vacuo to afford the debenylation product **4** (3.06 g, 98%) as a yellow solid. ¹H NMR (400 MHz, DMSO-*d*₆) δ 13.25 (s, 1H), 7.32 (t, *J* = 8.3 Hz, 1H), 6.72 (d, *J* = 8.3 Hz, 2H), 6.40 (s, 1H), 3.87 (s, 3H), 3.69 (s, 6H), 3.58 (s, 3H), 3.23 (s, 3H).

4.1.4 1,2,3,8-tetramethoxy-9H-xanthen-9-one (**5**).

To a solution of compound **4** (3.06 g) in a mixture of pyridine (38 mL) and water (38 mL) was added Me₄NOH (6.25 mL) at room temperature. The resulting solution was heated to reflux for 8 h and poured into a mixture of hydrochloric acid (1 mol/L, 200 mL) and ethyl acetate (200 mL) with vigorous stirring. The resulting mixture was separated into two phases. The organic phase was separated, washed with brine, dried over anhydrous Na₂SO₄, filtered and concentrated under reduced pressure successively. The residue was purified by flash column chromatography to afford tetra-methoxy xanthone **5** as a yellow solid (2.55 g, yield: 92%).

4.1.5 1-hydroxy-2,3,8-trimethoxy-9H-xanthen-9-one (**6**).

To a solution of xanthone **5** (1.05 g, 3.32 mmol) in dry DCM (80 mL) was added a solution of BCl₃ (1 mol/L, 3.5 mL) in DCM dropwise at -80 °C under argon. After 30 min, the reaction was quenched with dry methanol (100 mL) and concentrated in vacuo. The residue was washed with ether (10 mL) to afford the desired product **6** (920 mg, yield: 92%). ¹H NMR (400 MHz, DMSO-*d*₆) δ 13.23 (s, 1H), 7.75 (t, *J* = 8.4 Hz, 1H), 7.08 (d, *J* = 8.4 Hz, 1H), 6.99 (d, *J* = 8.4 Hz, 1H), 6.68 (s, 1H), 3.92 (s, 6H), 3.72 (s, 3H).

4.1.6 1,3-dihydroxy-2,8-dimethoxy-9H-xanthen-9-one (**7**).

Compound **6** (1.97 g, 6.52 mmol), piperidine (12 mL) and H₂O (3 mL) was added to a microwave vial (20 mL) and heated with microwave reactor (Biotage) with a programmed procedure of 120 °C for 24 h. After cooling to r.t., the clear red-brown solution was added to hydrochloric acid (1 mol/L, 100 mL) with vigorously stirring and yellow solids were precipitated. The mixture was filtered and the filter cake was washed with water, dried and purified by flash column chromatography to afford **7a** (850 mg, yield: 48%) and **7b** (930 mg, yield: 50%) as yellow solids respectively. **7a**: ¹H NMR (400 MHz, Chloroform-*d*) δ 12.20 (s, 1H), 11.87 (s, 1H), 7.57 (t, *J* = 8.3 Hz, 1H), 6.88 (dd, *J* = 8.4, 0.9 Hz, 1H), 6.78 (dd, *J* = 8.3, 0.9 Hz, 1H), 6.65 (s, 1H), 6.52 (s, 1H), 4.04 (s, 3H). ¹³C NMR (151 MHz, CDCl₃) δ 185.11, 161.16, 157.02, 156.17, 153.37, 152.79, 136.86, 129.76, 110.75, 107.26, 107.04, 102.79, 93.77, 61.04. **7b**: ¹H NMR (400 MHz, Chloroform-*d*) δ 13.49 (s, 1H), 7.59 (t, *J* = 8.4 Hz, 1H), 7.00 (dd, *J* = 8.5, 1.0 Hz, 1H), 6.79 (dd, *J* = 8.3, 1.0 Hz, 1H), 6.66 (s, 1H), 6.45 (s, 1H), 4.03 (s, 3H), 4.01 (s, 3H). ¹³C NMR (151 MHz, CDCl₃) δ 181.88, 160.53, 157.95, 155.89, 153.92, 152.37, 135.29, 129.62, 110.53, 109.84, 105.50, 104.38, 92.62, 60.92, 56.51.

4.2.7 1-hydroxy-2,8-dimethoxy-3-trifluoromethanesulfonyloxy-9H-xanthen-9-one (**8**).

To a solution of xanthone **7b** (0.900 g, 3.12 mmol) and pyridine (0.503 mL, 6.24 mmol) in dry DCM (30 mL) was added Tf₂O (0.630 mL, 3.75 mmol) dropwise at 0 °C. The reaction was completed after 1 h monitored by TLC. Then the mixture was quenched with hydrochloric acid (1 mol/L, 20 mL) and the organic phase was washed with saturated aqueous sodium bicarbonate solution and brine successively. After dried over with sodium sulfate, the solution was filtered and concentrated in vacuo. The residue was purified by flash column chromatography to afford the desired triflate **8** as a yellow solid (963 mg, yield: 73%). ¹H NMR (400 MHz, DMSO-*d*₆) δ 13.70 (s, 1H), 7.82

(t, $J = 8.4$ Hz, 1H), 7.24 (s, 1H), 7.12 (d, $J = 8.4$ Hz, 1H), 7.05 (d, $J = 8.4$ Hz, 1H), 3.94 (s, 3H), 3.93 (s, 3H). ^{13}C NMR (151 MHz, DMSO) δ 181.35, 160.26, 157.20, 154.88, 149.92, 145.90, 137.24, 134.21, 118.03 (q, $J = 320.3$ Hz), 109.63, 109.24, 109.15, 106.87, 99.85.

4.1.8 3-((diphenylmethylene)amino)-1-hydroxy-2,8-dimethoxy-9H-xanthen-9-one (**9**).

The triflate **8** (200 mg, 0.476 mmol), benzophenone imine (0.16 mL, 0.952 mmol), BINAP (44 mg, 0.071 mmol), Pd(OAc)₂ (11 mg, 0.048 mmol) and Cs₂CO₃ (217 mg, 0.666 mmol) were suspended in dioxane (5 mL) under argon and the resulting mixture was heated to reflux for 12 h. After cooling to r.t, the reaction mixture was diluted with ethyl acetate (10 mL), filtered through a celite bed and concentrated in vacuo successively. The residue was purified by flash column chromatography to afford the desired product **9** as a yellow solid (168 mg, yield: 78%).

4.1.9 3-amino-1-hydroxy-2,8-dimethoxy-9H-xanthen-9-one (**10**).

To a solution of compound **9** (168 mg, 0.372 mmol) in THF (10 mL) was added hydrochloric acid (4 mol/L, 4 mL). After 30 min, the reaction mixture was diluted with ethyl acetate (10 mL) and quenched with saturated aqueous sodium bicarbonate solution. The organic phase was separated, washed with brine, dried over sodium sulfate and concentrated in vacuo successively. The residue was crystallized in hexane/ethyl acetate to afford the desired amine **10** as a yellow solid (85 mg, yield: 80%). ^1H NMR (400 MHz, DMSO-*d*₆) δ 13.59 (s, 1H), 7.66 (t, $J = 8.4$ Hz, 1H), 7.03 (d, $J = 8.4$ Hz, 1H), 6.93 (d, $J = 8.4$ Hz, 1H), 6.43 (s, 2H), 6.12 (s, 1H), 3.88 (s, 3H), 3.72 (s, 3H). ^{13}C NMR (151 MHz, DMSO) δ 179.29, 159.81, 156.90, 153.27, 152.10, 149.89, 135.04, 127.73, 109.61, 109.11, 106.16, 100.09, 89.36, 59.10, 56.09. MS (ESI⁺) m/z 288.1 (M + H)⁺. HRMS (ESI⁺) m/z : 288.0858 (M + H)⁺ (calcd for C₁₅H₁₄NO₅⁺: 288.0866).

4.2 General synthetic procedure of compound **11a-11q**

To a solution of amine **10** (30 mg, 0.1 mmol) in dry pyridine (2 mL) was added substituted benzenesulfonyl chloride (1.5 - 2 eq.). The reaction mixture was kept at r.t overnight and poured into a mixture of hydrochloric acid (1 mol/L, 10 mL) and ethyl acetate (10 mL) with vigorous stirring. The organic phase was separated, washed with brine, dried over sodium sulfate and concentrated in vacuo successively. The residue was purified by flash column chromatography to afford the desired sulfonamides **11** as yellow solids (yield: 40% - 70%).

4.2.1 *N*-(1-hydroxy-2,8-dimethoxy-9-oxo-9H-xanthen-3-yl)benzenesulfonamide (**11a**).

Yield: 50%. ^1H NMR (400 MHz, DMSO-*d*₆) δ 13.34 (s, 1H), 10.57 (s, 1H), 7.95 (d, $J = 7.8$ Hz, 2H), 7.76 (t, $J = 8.3$ Hz, 1H), 7.63 (q, $J = 7.6$ Hz, 3H), 7.13 (d, $J = 8.4$ Hz, 1H), 6.99 (d, $J = 8.5$ Hz, 1H), 6.94 (s, 1H), 3.90 (s, 3H), 3.62 (d, $J = 1.8$ Hz, 3H). MS (ESI) m/z 426.1 (M - H)⁻

4.2.2 *N*-(1-hydroxy-2,8-dimethoxy-9-oxo-9H-xanthen-3-yl)-4-methylbenzenesulfonamide (**11b**).

Yield: 70%. ^1H NMR (400 MHz, DMSO-*d*₆) δ 13.33 (s, 1H), 10.46 (s, 1H), 7.83 (d, $J = 8.0$ Hz, 2H), 7.75 (t, $J = 8.5$ Hz, 1H), 7.41 (d, $J = 8.0$ Hz, 2H), 7.12 (d, $J = 8.6$ Hz, 1H), 6.99 (d, $J = 8.4$ Hz, 1H), 6.92 (s, 1H), 3.90 (s, 3H), 3.64 (s, 3H), 2.34 (s, 3H). ^{13}C NMR (151 MHz, DMSO) δ 180.84, 160.03, 157.18, 153.36, 150.42, 143.81, 138.02, 136.66, 136.37, 131.64, 129.83, 126.60, 109.61, 109.27, 106.48, 105.20, 94.94, 60.14, 56.22, 20.89.

4.2.3 *N*-(1-hydroxy-2,8-dimethoxy-9-oxo-9H-xanthen-3-yl)-4-(trifluoromethyl)benzenesulfonamide (**11d**).

Yield: 67%. ^1H NMR (400 MHz, DMSO-*d*₆) δ 13.36 (s, 1H), 10.79 (s, 1H), 8.16 (d, $J = 8.2$ Hz, 2H), 8.03 (d, $J = 8.3$ Hz, 2H), 7.76 (t, $J = 8.4$ Hz, 1H), 7.12 (d, $J = 8.5$ Hz, 1H), 7.00 (d, $J = 8.5$ Hz, 1H), 6.96 (s, 1H), 3.91 (s, 3H), 3.62 (s, 3H). ^{13}C NMR (151 MHz, DMSO) δ 180.95, 160.08, 157.22, 153.53, 150.41, 143.51, 137.26, 136.51, 132.85 (q, $J = 32.4$ Hz), 132.19, 127.57, 126.73, 125.93, 123.22 (q, $J = 273.1$ Hz), 109.63, 109.28, 106.53, 105.73, 95.79, 60.14, 56.25.

4.2.4 *N*-(1-hydroxy-2,8-dimethoxy-9-oxo-9H-xanthen-3-yl)-2,5-bis(trifluoromethyl)benzenesulfonamide (**11e**).

Yield: 64%. ^1H NMR (400 MHz, DMSO-*d*₆) δ 13.41 (s, 1H), 11.10 (brs, 1H), 8.51 (s, 1H), 8.29 (s, 2H), 7.76 (t, $J = 8.4$ Hz, 1H), 7.11 (d, $J = 8.5$ Hz, 1H), 7.00 (d, $J = 8.4$ Hz, 1H), 6.84 (s, 1H), 3.91 (s, 3H), 3.62 (s, 3H). ^{13}C NMR (151 MHz, DMSO) δ 181.07, 160.11, 157.23, 153.64, 150.13, 140.31, 136.62, 133.14, 133.02 (q, $J = 37.6$ Hz), 130.56, 130.23, 129.70 (q, $J = 33.5, 31.7$ Hz), 127.01, 122.47 (q, $J = 273.5$ Hz), 121.95 (q, $J = 274.0, 273.4$ Hz), 109.61, 109.27, 106.55, 106.30, 97.85, 59.97, 56.26.

4.2.5 *N*-(1-hydroxy-2,8-dimethoxy-9-oxo-9*H*-xanthen-3-yl)-3-(trifluoromethoxy)benzenesulfonamide (**II**f).

Yield: 52%. ¹H NMR (400 MHz, DMSO-*d*₆) δ 13.35 (s, 1H), 10.70 (s, 1H), 7.97 (d, *J* = 7.8 Hz, 1H), 7.92 (s, 1H), 7.84 – 7.67 (m, 3H), 7.12 (d, *J* = 8.4 Hz, 1H), 6.99 (d, *J* = 8.5 Hz, 1H), 6.95 (s, 1H), 3.91 (s, 3H), 3.60 (s, 3H). ¹³C NMR (151 MHz, DMSO) δ 180.95, 160.09, 157.23, 153.52, 150.38, 148.22, 141.57, 137.23, 136.51, 132.31, 131.97, 126.08, 125.67, 119.78 (q, *J* = 257.4 Hz), 118.98, 109.62, 109.25, 106.52, 105.76, 96.06, 60.07, 56.25.

4.2.6 4-fluoro-*N*-(1-hydroxy-2,8-dimethoxy-9-oxo-9*H*-xanthen-3-yl)benzenesulfonamide (**II**g).

Yield: 56%. ¹H NMR (400 MHz, DMSO-*d*₆) δ 13.35 (s, 1H), 10.57 (s, 1H), 8.03 (dd, *J* = 8.7, 5.1 Hz, 2H), 7.75 (t, *J* = 8.4 Hz, 1H), 7.47 (t, *J* = 8.8 Hz, 2H), 7.12 (d, *J* = 8.5 Hz, 1H), 6.99 (d, *J* = 8.4 Hz, 1H), 6.95 (s, 1H), 3.91 (s, 3H), 3.64 (s, 3H). ¹³C NMR (151 MHz, DMSO) δ 180.91, 164.49 (d, *J* = 252.3 Hz), 160.05, 157.21, 153.44, 150.44, 137.66, 136.45, 135.94, 131.90, 129.72 (d, *J* = 9.3 Hz), 116.68 (d, *J* = 22.9 Hz), 109.61, 109.27, 106.49, 105.45, 95.37, 60.17, 56.23.

4.2.7 4-chloro-*N*-(1-hydroxy-2,8-dimethoxy-9-oxo-9*H*-xanthen-3-yl)benzenesulfonamide (**II**h).

Yield: 65%. ¹H NMR (400 MHz, DMSO-*d*₆) δ 13.35 (s, 1H), 10.63 (s, 1H), 7.95 (d, *J* = 8.4 Hz, 2H), 7.77 (t, *J* = 8.4 Hz, 1H), 7.70 (d, *J* = 8.5 Hz, 2H), 7.13 (d, *J* = 8.5 Hz, 1H), 7.00 (d, *J* = 8.6 Hz, 1H), 6.93 (s, 1H), 3.91 (s, 3H), 3.64 (s, 3H).

4.2.8 4-bromo-*N*-(1-hydroxy-2,8-dimethoxy-9-oxo-9*H*-xanthen-3-yl)benzenesulfonamide (**II**i).

Yield: 68%. ¹H NMR (400 MHz, DMSO-*d*₆) δ 13.36 (s, 1H), 10.65 (s, 1H), 7.87 (dd, *J* = 3.7, 1.8 Hz, 4H), 7.76 (t, *J* = 8.2 Hz, 1H), 7.12 (d, *J* = 8.3 Hz, 1H), 6.99 (d, *J* = 8.3 Hz, 1H), 6.93 (s, 1H), 3.90 (s, 3H), 3.64 (s, 3H). ¹³C NMR (151 MHz, DMSO) δ 180.89, 160.03, 157.18, 153.46, 150.41, 138.80, 137.51, 136.44, 132.54, 131.93, 128.55, 127.27, 109.60, 109.26, 106.47, 105.51, 95.39, 60.17, 56.23.

4.2.9 *N*-(1-hydroxy-2,8-dimethoxy-9-oxo-9*H*-xanthen-3-yl)-4-iodobenzenesulfonamide (**II**j).

Yield: 65%. ¹H NMR (400 MHz, DMSO-*d*₆) δ 13.36 (s, 1H), 10.61 (s, 1H), 8.02 (d, *J* = 8.5 Hz, 2H), 7.75 (t, *J* = 8.1 Hz, 1H), 7.70 (d, *J* = 8.6 Hz, 2H), 7.11 (d, *J* = 8.5 Hz, 1H), 6.99 (d, *J* = 8.4 Hz, 1H), 6.92 (s, 1H), 3.90 (s, 3H), 3.65 (s, 3H). ¹³C NMR (151 MHz, DMSO) δ 180.90, 160.06, 157.21, 153.46, 150.43, 139.17, 138.34, 137.58, 136.43, 131.91, 128.18, 109.63, 109.28, 106.50, 105.49, 101.78, 95.32, 60.18, 56.24.

4.2.10 *N*-(1-hydroxy-2,8-dimethoxy-9-oxo-9*H*-xanthen-3-yl)naphthalene-1-sulfonamide (**II**m).

Yield: 61%. ¹H NMR (400 MHz, DMSO-*d*₆) δ 13.28 (s, 1H), 10.92 (s, 1H), 8.87 (d, *J* = 9.4 Hz, 1H), 8.34 (d, *J* = 7.5 Hz, 1H), 8.28 (d, *J* = 8.5 Hz, 1H), 8.10 (d, *J* = 7.5 Hz, 1H), 7.83 – 7.61 (m, 4H), 7.08 (d, *J* = 8.1 Hz, 1H), 6.96 (d, *J* = 8.8 Hz, 1H), 6.86 (s, 1H), 3.87 (s, 3H), 3.50 (s, 3H). ¹³C NMR (151 MHz, DMSO) δ 180.80, 160.02, 157.15, 153.35, 150.37, 137.66, 136.36, 134.87, 134.02, 133.75, 131.56, 129.73, 129.05, 128.33, 127.19, 127.12, 124.45, 124.28, 109.58, 109.24, 106.47, 105.16, 94.91, 60.01, 56.20.

4.2.11 *N*-(1-hydroxy-2,8-dimethoxy-9-oxo-9*H*-xanthen-3-yl)naphthalene-2-sulfonamide (**II**n).

Yield: 55%. ¹H NMR (400 MHz, DMSO-*d*₆) δ 13.32 (s, 1H), 10.65 (s, 1H), 8.65 (s, 1H), 8.21 (d, *J* = 8.0 Hz, 1H), 8.15 (d, *J* = 8.7 Hz, 1H), 8.02 (d, *J* = 8.0 Hz, 1H), 7.97 (d, *J* = 8.8 Hz, 1H), 7.79 – 7.62 (m, 3H), 7.10 (d, *J* = 8.6 Hz, 1H), 7.00 (s, 1H), 6.96 (d, *J* = 8.5 Hz, 1H), 3.88 (s, 3H), 3.64 (s, 3H). ¹³C NMR (151 MHz, DMSO) δ 180.87, 160.03, 157.19, 153.39, 150.43, 137.84, 136.57, 136.37, 134.34, 131.80, 131.42, 129.69, 129.29, 129.16, 127.86, 127.78, 121.80, 109.61, 109.26, 106.46, 105.34, 95.19, 60.17, 56.21.

4.2.12 *N*-(1-hydroxy-2,8-dimethoxy-9-oxo-9*H*-xanthen-3-yl)-[1,1'-biphenyl]-4-sulfonamide (**II**o).

Yield: 70%. ¹H NMR (400 MHz, DMSO-*d*₆) δ 13.35 (s, 1H), 10.61 (s, 1H), 8.03 (d, *J* = 8.2 Hz, 2H), 7.92 (d, *J* = 8.2 Hz, 2H), 7.79 – 7.65 (m, 3H), 7.55 – 7.37 (m, 3H), 7.12 (d, *J* = 9.1 Hz, 1H), 7.02 – 6.94 (m, 2H), 3.89 (s, 3H), 3.68 (s, 3H). ¹³C NMR (151 MHz, DMSO) δ 180.80, 159.98, 157.13, 153.37, 150.40, 144.64, 138.21, 137.99, 137.82, 136.33, 131.68, 128.94, 128.50, 127.50, 127.19, 126.93, 109.55, 109.21, 106.42, 105.27, 94.99, 60.12, 56.16.

4.2.13 4-(*tert*-butyl)-*N*-(1-hydroxy-2,8-dimethoxy-9-oxo-9*H*-xanthen-3-yl)benzenesulfonamide (**II**p).

Yield: 59%. ¹H NMR (400 MHz, DMSO-*d*₆) δ 13.34 (s, 1H), 10.51 (s, 1H), 7.89 (d, *J* = 8.2 Hz, 2H), 7.74 (t, *J* = 8.4 Hz, 1H), 7.64 (d, *J* = 8.2

Hz, 2H), 7.11 (d, $J = 8.5$ Hz, 1H), 6.97 (t, $J = 4.5$ Hz, 2H), 3.89 (s, 3H), 3.64 (s, 3H), 1.26 (s, 9H).

4.2.14 4-cyclohexyl-*N*-(1-hydroxy-2,8-dimethoxy-9-oxo-9*H*-xanthen-3-yl)benzenesulfonamide (**11q**).

Yield: 60%. ^1H NMR (400 MHz, DMSO- d_6) δ 13.34 (s, 1H), 10.48 (s, 1H), 7.87 (d, $J = 8.2$ Hz, 2H), 7.73 (td, $J = 8.4, 2.3$ Hz, 1H), 7.46 (d, $J = 8.1$ Hz, 2H), 7.10 (d, $J = 8.5$ Hz, 1H), 7.01 – 6.94 (m, 2H), 3.89 (s, 3H), 3.63 (s, 3H), 2.60 – 2.53 (m, 1H), 1.86 – 1.61 (m, 5H), 1.34 (h, $J = 12.4$ Hz, 4H), 1.24 – 1.11 (m, 1H). ^{13}C NMR (151 MHz, DMSO) δ 180.86, 160.04, 157.19, 153.39, 153.27, 150.45, 138.01, 137.10, 136.37, 131.65, 127.69, 126.70, 109.62, 109.27, 106.47, 105.24, 95.00, 60.09, 56.22, 43.45, 33.28, 26.00, 25.29.

4.2.15 *N*-(1-hydroxy-2,8-dimethoxy-9-oxo-9*H*-xanthen-3-yl)-4-(pyrrolidin-1-yl)benzenesulfonamide (**11r**).

11j (50 mg, 0.09 mmol), Pd₂dba₃ (8.3 mg, 0.009 mmol), BINAP (16.9 mg, 0.027 mmol), pyrrolidine (0.022 mL, 0.271 mmol), and *t*-BuONa (43 mg, 0.452 mmol) were suspended in NMP (2 mL) under argon and the resulting mixture was heated to 80°C for 8 h. After cooling to r.t., the reaction mixture was diluted with ethyl acetate (10 mL), filtered through a celite bed and concentrated in vacuo successively. The residue was purified by flash column chromatography to afford the desired product **11r** as a yellow solid (25 mg, yield: 54%).

4.2.16 *N*-(1-hydroxy-2,8-dimethoxy-9-oxo-9*H*-xanthen-3-yl)-4-(piperidin-1-yl)benzenesulfonamide (**11s**).

11j (50 mg, 0.09 mmol), Pd₂dba₃ (8.3 mg, 0.009 mmol), BINAP (16.9 mg, 0.027 mmol), piperidine (0.025 mL, 0.271 mmol), and *t*-BuONa (43 mg, 0.452 mmol) were suspended in NMP (2 mL) under argon and the resulting mixture was heated to 80°C for 8 h. After cooling to r.t., the reaction mixture was diluted with ethyl acetate (10 mL), filtered through a celite bed and concentrated in vacuo successively. The residue was purified by flash column chromatography to afford the desired product **11s** as a yellow solid (30 mg, yield: 65%).

4.3 General synthetic procedure of compound **12a-12s**

To a solution of compound **11** in dry DCM ($c = 0.1$ mol/L) was added a solution of BBr₃ (1 mol/L, 5 eq.) in DCM at 0 °C. The reaction solution was quenched with dry methanol after 2 h and concentrated in vacuo. The residue was recrystallized from methanol/ethyl acetate to afford the desired sulfonamides **12** as yellow solids (yield: 30% - 50%).

4.3.1 *N*-(1,2,8-trihydroxy-9-oxo-9*H*-xanthen-3-yl)benzenesulfonamide (**12a**).

Yield: 48%. ^1H NMR (400 MHz, DMSO- d_6) δ 11.73 (s, 1H), 11.60 (s, 1H), 10.39 (s, 1H), 9.68 (s, 1H), 7.98 (d, $J = 7.7$ Hz, 2H), 7.73 – 7.55 (m, 4H), 7.03 (d, $J = 8.5$ Hz, 1H), 6.98 (s, 1H), 6.78 (d, $J = 8.3$ Hz, 1H). ^{13}C NMR (151 MHz, DMSO) δ 184.24, 160.05, 155.74, 148.58, 146.89, 139.73, 137.41, 135.07, 133.28, 130.13, 129.37, 126.61, 110.12, 107.18, 106.89, 103.66, 96.00. MS (ESI) m/z 398.0 (M - H)⁻. HRMS (ESI) m/z : 398.035 (M - H)⁻ (calcd for C₁₉H₁₃NO₇S⁻: 398.0340).

4.3.2 4-methyl-*N*-(1,2,8-trihydroxy-9-oxo-9*H*-xanthen-3-yl)benzenesulfonamide (**12b**).

Yield: 50%. ^1H NMR (400 MHz, DMSO- d_6) δ 11.73 (s, 1H), 11.58 (s, 1H), 10.25 (s, 1H), 9.64 (s, 1H), 7.86 (d, $J = 8.2$ Hz, 2H), 7.69 (t, $J = 8.3$ Hz, 1H), 7.41 (d, $J = 7.9$ Hz, 2H), 7.02 (d, $J = 8.2$ Hz, 1H), 6.97 (s, 1H), 6.78 (d, $J = 8.3$ Hz, 1H), 2.35 (s, 3H). ^{13}C NMR (151 MHz, DMSO) δ 184.20, 160.05, 155.72, 148.62, 146.86, 143.76, 137.36, 136.83, 135.22, 129.97, 129.78, 126.69, 110.11, 107.15, 106.87, 103.56, 95.81, 20.90. MS (ESI) m/z 411.7 (M - H)⁻. HRMS (ESI) m/z : 412.0492 (M - H)⁻ (calcd for C₂₀H₁₅NO₇S⁻: 412.0496).

4.3.3 1-phenyl-*N*-(1,2,8-trihydroxy-9-oxo-9*H*-xanthen-3-yl)methanesulfonamide (**12c**).

Yield: 30%. ^1H NMR (400 MHz, DMSO- d_6) δ 11.79 (s, 1H), 11.62 (s, 1H), 9.74 (s, 1H), 9.45 (s, 1H), 7.71 (t, $J = 8.5$ Hz, 1H), 7.41 – 7.24 (m, 5H), 7.03 (d, $J = 8.5$ Hz, 1H), 6.89 (s, 1H), 6.80 (d, $J = 8.3$ Hz, 1H), 4.71 (s, 2H). ^{13}C NMR (151 MHz, DMSO) δ 184.15, 160.09, 155.75, 148.76, 146.74, 137.40, 136.26, 130.96, 129.50, 128.83, 128.27, 128.27, 110.10, 107.14, 106.82, 103.32, 95.98, 58.30. MS (ESI) m/z 411.8 (M - H)⁻. HRMS (ESI) m/z : 412.0487 (M - H)⁻ (calcd for C₂₀H₁₅NO₇S⁻: 412.0496).

4.3.4 4-(trifluoromethyl)-*N*-(1,2,8-trihydroxy-9-oxo-9*H*-xanthen-3-yl)benzenesulfonamide (**12d**).

Yield: 45%. ^1H NMR (400 MHz, DMSO- d_6) δ 11.71 (s, 1H), 11.62 (s, 1H), 10.64 (s, 1H), 9.67 (s, 1H), 8.17 (d, $J = 8.2$ Hz, 2H), 8.01 (d, $J = 8.2$ Hz, 2H), 7.71 (t, $J = 8.3$ Hz, 1H), 7.03 (d, $J = 8.5$ Hz, 1H), 7.00 (s, 1H), 6.79 (d, $J = 8.3$ Hz, 1H). ^{13}C NMR (151 MHz, DMSO) δ 184.28, 160.02, 155.72, 148.43, 146.97, 143.73, 134.35, 137.43, 132.67 (q, $J = 32.4$ Hz), 130.74, 127.56, 126.54, 126.52, 123.20 (q, $J = 272.9$ Hz),

110.10, 107.12, 106.86, 104.03, 96.91. MS (ESI) m/z 466.0 (M - H)⁻. HRMS (ESI) m/z : 466.0207 (M - H)⁻ (calcd for C₂₀H₁₂F₃NO₇S⁻: 466.0214).

4.3.5 2,5-bis(trifluoromethyl)-*N*-(1,2,8-trihydroxy-9-oxo-9*H*-xanthen-3-yl)benzenesulfonamide (**12e**).

Yield: 46%. ¹H NMR (400 MHz, DMSO-*d*₆) δ 11.64 (s, 1H), 11.62 (s, 1H), 10.93 (s, 1H), 9.81 (s, 1H), 8.49 (s, 1H), 8.23 (s, 2H), 7.65 (t, *J* = 8.3 Hz, 1H), 6.96 (d, *J* = 8.4 Hz, 1H), 6.86 (s, 1H), 6.74 (d, *J* = 8.3 Hz, 1H). ¹³C NMR (151 MHz, DMSO) δ 184.40, 160.03, 155.73, 148.09, 147.10, 140.42, 137.51, 132.9 (q, *J* = 33.4 Hz), 131.80, 130.35, 130.11, 130.06, 129.67 (q, *J* = 35.0 Hz), 126.87, 122.43 (q, *J* = 273.8 Hz), 121.93 (q, *J* = 274.9 Hz), 110.10, 107.11, 106.88, 104.55, 98.8. MS (ESI) m/z 534.0 (M - H)⁻. HRMS (ESI) m/z : 534.0084 (M - H)⁻ (calcd for C₂₁H₁₁F₆NO₇S⁻: 534.0088).

4.3.6 3-(trifluoromethoxy)-*N*-(1,2,8-trihydroxy-9-oxo-9*H*-xanthen-3-yl)benzenesulfonamide (**12f**).

Yield: 48%. ¹H NMR (400 MHz, DMSO-*d*₆) δ 11.71 (s, 1H), 11.61 (s, 1H), 10.57 (s, 1H), 9.71 (s, 1H), 8.00 (d, *J* = 7.8 Hz, 1H), 7.95 (s, 1H), 7.81 – 7.65 (m, 3H), 7.02 (d, *J* = 8.4 Hz, 1H), 6.98 (s, 1H), 6.79 (d, *J* = 8.3 Hz, 1H). ¹³C NMR (151 MHz, DMSO) δ 184.35, 160.09, 155.79, 148.47, 148.16, 147.03, 141.85, 137.51, 131.84, 130.80, 125.93, 125.72, 122.35, 119.79 (q, *J* = 258.0 Hz), 119.13, 110.16, 107.16, 106.91, 104.08, 96.93. MS (ESI) m/z 482.0 (M - H)⁻. HRMS (ESI) m/z : 482.0152 (M - H)⁻ (calcd for C₂₀H₁₂F₃NO₈S⁻: 482.0163).

4.3.7 4-fluoro-*N*-(1,2,8-trihydroxy-9-oxo-9*H*-xanthen-3-yl)benzenesulfonamide (**12g**).

Yield: 45%. ¹H NMR (400 MHz, DMSO-*d*₆) δ 11.73 (s, 1H), 11.60 (s, 1H), 10.38 (s, 1H), 9.66 (s, 1H), 8.05 (dd, *J* = 8.7, 5.3 Hz, 2H), 7.70 (t, *J* = 8.4 Hz, 1H), 7.46 (t, *J* = 8.7 Hz, 2H), 7.03 (d, *J* = 8.4 Hz, 1H), 6.99 (s, 1H), 6.79 (d, *J* = 8.2 Hz, 1H). ¹³C NMR (151 MHz, DMSO) δ 184.22, 164.42 (d, *J* = 252.2 Hz), 160.02, 155.69, 148.52, 146.89, 137.38, 136.09, 134.79, 130.32, 129.74 (d, *J* = 10.0 Hz), 116.50 (d, *J* = 22.7 Hz), 110.08, 107.10, 106.84, 103.76, 96.33. MS (ESI) m/z 416.0 (M - H)⁻. HRMS (ESI) m/z : 416.0237 (M - H)⁻ (calcd for C₁₉H₁₂FNO₇S⁻: 416.0246).

4.3.8 4-chloro-*N*-(1,2,8-trihydroxy-9-oxo-9*H*-xanthen-3-yl)benzenesulfonamide (**12h**).

Yield: 43%. ¹H NMR (400 MHz, DMSO-*d*₆) δ 11.72 (s, 1H), 11.61 (s, 1H), 10.46 (s, 1H), 9.68 (s, 1H), 7.97 (d, *J* = 8.6 Hz, 2H), 7.75 – 7.65 (m, 3H), 7.03 (d, *J* = 8.4 Hz, 1H), 6.98 (s, 1H), 6.79 (d, *J* = 8.3 Hz, 1H). ¹³C NMR (151 MHz, DMSO) δ 184.25, 160.02, 155.71, 148.47, 146.94, 138.57, 138.10, 137.40, 134.57, 130.47, 129.44, 128.54, 110.09, 107.11, 106.85, 103.88, 96.54. MS (ESI) m/z 432.0 (M - H)⁻. HRMS (ESI) m/z : 431.9941 (M - H)⁻ (calcd for C₁₉H₁₂ClNO₇S⁻: 431.9950).

4.3.9 4-bromo-*N*-(1,2,8-trihydroxy-9-oxo-9*H*-xanthen-3-yl)benzenesulfonamide (**12i**).

Yield: 43%. ¹H NMR (400 MHz, DMSO-*d*₆) δ 11.73 (s, 1H), 11.61 (s, 1H), 10.49 (s, 1H), 9.68 (s, 1H), 7.93 – 7.80 (m, 4H), 7.70 (t, *J* = 8.3 Hz, 1H), 7.03 (d, *J* = 8.2 Hz, 1H), 6.97 (s, 1H), 6.79 (d, *J* = 7.9 Hz, 1H). ¹³C NMR (151 MHz, DMSO) δ 184.28, 160.05, 155.74, 148.51, 146.94, 139.04, 137.44, 134.64, 132.42, 130.49, 128.63, 127.18, 110.13, 107.17, 106.90, 103.90, 96.53. MS (ESI) m/z 476.0 (M - H)⁻. HRMS (ESI) m/z : 475.9426 (M - H)⁻ (calcd for C₁₉H₁₂BrNO₇S⁻: 475.9445).

4.3.10 4-iodo-*N*-(1,2,8-trihydroxy-9-oxo-9*H*-xanthen-3-yl)benzenesulfonamide (**12j**).

Yield: 41%. ¹H NMR (400 MHz, DMSO-*d*₆) δ 11.73 (s, 1H), 11.61 (s, 1H), 9.66 (s, 1H), 8.66 (s, 1H), 8.00 (d, *J* = 8.2 Hz, 2H), 7.75 – 7.65 (m, 3H), 7.03 (d, *J* = 7.8 Hz, 1H), 6.97 (s, 1H), 6.79 (d, *J* = 8.0 Hz, 1H). ¹³C NMR (151 MHz, DMSO) δ 184.24, 160.01, 155.71, 148.50, 146.91, 139.34, 138.17, 137.39, 134.68, 130.38, 128.22, 110.08, 107.12, 106.85, 103.82, 101.64, 96.39. MS (ESI) m/z 523.8 (M - H)⁻. HRMS (ESI) m/z : 523.9287 (M - H)⁻ (calcd for Chemical Formula: C₁₉H₁₂INO₇S⁻: 523.9306).

4.3.11 4-cyano-*N*-(1,2,8-trihydroxy-9-oxo-9*H*-xanthen-3-yl)benzenesulfonamide (**12k**).

Yield: 34%. ¹H NMR (400 MHz, DMSO-*d*₆) δ 11.70 (s, 1H), 11.62 (s, 1H), 10.65 (s, 1H), 9.68 (s, 1H), 8.16 – 8.06 (m, 4H), 7.70 (t, *J* = 8.3 Hz, 1H), 7.03 (d, *J* = 8.4 Hz, 1H), 6.98 (s, 1H), 6.79 (d, *J* = 8.3 Hz, 1H). ¹³C NMR (151 MHz, DMSO) δ 184.37, 160.09, 155.78, 148.44, 147.10, 143.85, 137.53, 134.16, 133.49, 130.96, 127.37, 117.46, 115.60, 110.16, 107.17, 106.92, 104.21, 97.26. MS (ESI) m/z 422.9 (M - H)⁻. HRMS (ESI) m/z : 423.0285 (M - H)⁻ (calcd for Chemical Formula: C₂₀H₁₂N₂O₇S⁻: 423.0292).

4.3.12 3-cyano-*N*-(1,2,8-trihydroxy-9-oxo-9*H*-xanthen-3-yl)benzenesulfonamide (**12l**)

Yield: 33%. ¹H NMR (400 MHz, DMSO-*d*₆) δ 11.72 (s, 1H), 11.62 (s, 1H), 10.56 (s, 1H), 9.69 (s, 1H), 8.44 (s, 1H), 8.25 (d, *J* = 8.0 Hz, 1H), 8.15 (d, *J* = 7.8 Hz, 1H), 7.82 (t, *J* = 7.8 Hz, 1H), 7.71 (t, *J* = 8.8 Hz, 1H), 7.04 (d, *J* = 8.5 Hz, 1H), 7.00 (s, 1H), 6.79 (d, *J* = 8.3 Hz, 1H). ¹³C NMR (151 MHz, DMSO) δ 184.37, 160.09, 155.80, 148.50, 147.04, 141.21, 137.51, 136.72, 131.01, 130.90, 130.76, 130.30, 117.33, 112.51, 110.15, 107.18, 106.94, 104.19, 97.29. MS (ESI) *m/z* 422.8 (M - H)⁻. HRMS (ESI) *m/z*: 423.0278 (M - H)⁻ (calcd for Chemical Formula: C₂₀H₁₂N₂O₇S⁻: 423.0292).

4.3.13 *N*-(1,2,8-trihydroxy-9-oxo-9*H*-xanthen-3-yl)naphthalene-1-sulfonamide (**12m**)

Yield: 42%. ¹H NMR (400 MHz, DMSO-*d*₆) δ 11.70 (s, 1H), 11.54 (s, 1H), 10.73 (s, 1H), 9.62 (s, 1H), 8.84 (d, *J* = 8.6 Hz, 1H), 8.33 (d, *J* = 7.5 Hz, 1H), 8.27 (d, *J* = 8.3 Hz, 1H), 8.10 (d, *J* = 8.4 Hz, 1H), 7.79 – 7.59 (m, 4H), 6.99 (d, *J* = 8.5 Hz, 1H), 6.92 (s, 1H), 6.76 (d, *J* = 8.1 Hz, 1H). ¹³C NMR (151 MHz, DMSO) δ 184.11, 159.98, 155.64, 148.47, 146.72, 137.29, 135.00, 134.69, 134.36, 133.69, 129.92, 129.35, 128.91, 128.20, 127.19, 127.01, 124.37, 124.32, 110.04, 107.08, 106.79, 103.44, 95.77. MS (ESI) *m/z* 447.8 (M - H)⁻. HRMS (ESI) *m/z*: 448.0478 (M - H)⁻ (calcd for Chemical Formula: C₂₃H₁₅NO₇S⁻: 448.0496).

4.3.14 *N*-(1,2,8-trihydroxy-9-oxo-9*H*-xanthen-3-yl)naphthalene-2-sulfonamide (**12n**)

Yield: 41%. ¹H NMR (400 MHz, DMSO-*d*₆) δ 11.70 (s, 1H), 11.57 (s, 1H), 10.44 (s, 1H), 9.66 (s, 1H), 8.66 (s, 1H), 8.20 (d, *J* = 8.5 Hz, 1H), 8.13 (d, *J* = 8.8 Hz, 1H), 8.06 – 7.94 (m, 2H), 7.76 – 7.61 (m, 3H), 7.05 (s, 1H), 7.00 (d, *J* = 7.6 Hz, 1H), 6.76 (d, *J* = 8.2 Hz, 1H). ¹³C NMR (151 MHz, DMSO) δ 184.18, 159.98, 155.67, 148.52, 146.84, 137.32, 136.73, 134.97, 134.29, 131.37, 130.20, 129.50, 129.22, 129.04, 127.78, 127.71, 127.64, 121.89, 110.04, 107.09, 106.82, 103.67, 96.20. MS (ESI) *m/z* 447.9 (M - H)⁻. HRMS (ESI) *m/z*: 448.0478 (M - H)⁻ (calcd for Chemical Formula: C₂₃H₁₅NO₇S⁻: 448.0496).

4.3.15 *N*-(1,2,8-trihydroxy-9-oxo-9*H*-xanthen-3-yl)-[1,1'-biphenyl]-4-sulfonamide (**12o**)

Yield: 48%. ¹H NMR (400 MHz, DMSO-*d*₆) δ 11.73 (s, 1H), 11.60 (s, 1H), 10.41 (s, 1H), 9.68 (s, 1H), 8.06 (d, *J* = 8.2 Hz, 2H), 7.91 (d, *J* = 8.1 Hz, 2H), 7.74 – 7.66 (m, 3H), 7.53 – 7.38 (m, 3H), 7.06 – 7.00 (m, 2H), 6.78 (d, *J* = 8.3 Hz, 1H). ¹³C NMR (151 MHz, DMSO) δ 184.2, 160.0, 155.7, 148.6, 146.9, 144.6, 138.5, 138.1, 137.4, 135.1, 130.1, 129.0, 128.5, 127.5, 127.3, 127.0, 110.1, 107.2, 106.9, 103.7, 95.9. MS (ESI) *m/z* 473.9 (M - H)⁻. HRMS (ESI) *m/z*: 474.0631 (M - H)⁻ (calcd for Chemical Formula: C₂₃H₁₄NO₇S⁻: 474.0653).

4.3.16 4-(*tert*-butyl)-*N*-(1,2,8-trihydroxy-9-oxo-9*H*-xanthen-3-yl)benzenesulfonamide (**12p**)

Yield: 45%. ¹H NMR (400 MHz, DMSO-*d*₆) δ 11.73 (s, 1H), 11.59 (s, 1H), 10.30 (s, 1H), 9.67 (brs, 1H), 7.92 (d, *J* = 8.3 Hz, 2H), 7.73 – 7.56 (m, 3H), 7.06 – 6.99 (m, 2H), 6.78 (d, *J* = 8.4 Hz, 1H), 1.27 (s, 9H). ¹³C NMR (151 MHz, DMSO) δ 184.19, 160.05, 156.33, 155.72, 148.70, 146.86, 137.36, 136.96, 135.34, 129.77, 126.54, 126.25, 110.12, 107.17, 106.87, 103.49, 95.45, 34.84, 30.59. MS (ESI) *m/z* 454.1 (M - H)⁻. HRMS (ESI) *m/z*: 454.0953 (M - H)⁻ (calcd for Chemical Formula: C₂₃H₂₁NO₇S⁻: 454.0966).

4.3.17 4-cyclohexyl-*N*-(1,2,8-trihydroxy-9-oxo-9*H*-xanthen-3-yl)benzenesulfonamide (**12q**)

Yield: 41%. ¹H NMR (400 MHz, DMSO-*d*₆) δ 11.73 (s, 1H), 11.59 (s, 1H), 10.28 (s, 1H), 9.66 (s, 1H), 7.90 (d, *J* = 8.0 Hz, 2H), 7.68 (t, *J* = 8.4 Hz, 1H), 7.46 (d, *J* = 8.1 Hz, 2H), 7.06 – 6.98 (m, 2H), 6.77 (d, *J* = 8.3 Hz, 1H), 2.62 – 2.53 (m, 1H), 1.82 – 1.61 (m, 5H), 1.47 – 1.12 (m, 5H). ¹³C NMR (151 MHz, DMSO) δ 184.20, 160.06, 155.73, 153.21, 148.70, 146.88, 137.36, 137.24, 135.35, 129.81, 127.64, 126.79, 110.12, 107.17, 106.88, 103.51, 95.55, 43.45, 33.28, 26.01, 25.30. MS (ESI) *m/z* 480.1 (M - H)⁻. HRMS (ESI) *m/z*: 480.1103 (M - H)⁻ (calcd for Chemical Formula: C₂₅H₂₃NO₇S⁻: 480.1122).

4.3.18 4-(pyrrolidin-1-yl)-*N*-(1,2,8-trihydroxy-9-oxo-9*H*-xanthen-3-yl)benzenesulfonamide (**12r**)

Yield: 33%. ¹H NMR (400 MHz, DMSO-*d*₆) δ 11.77 (s, 1H), 11.56 (s, 1H), 9.77 (s, 1H), 7.76 – 7.60 (m, 3H), 7.04 (d, *J* = 8.5 Hz, 1H), 6.98 (s, 1H), 6.78 (d, *J* = 8.3 Hz, 1H), 6.59 (d, *J* = 8.8 Hz, 2H), 3.25 (t, *J* = 6.6 Hz, 4H), 1.92 (d, *J* = 6.6 Hz, 4H). ¹³C NMR (151 MHz, DMSO) δ 184.09, 160.06, 155.70, 150.22, 148.85, 146.65, 137.29, 136.04, 129.26, 128.62, 123.31, 110.86, 110.11, 107.16, 106.85, 103.09, 94.92, 47.15, 24.80. MS (ESI) *m/z* 466.8 (M - H)⁻. HRMS (ESI) *m/z*: 467.0899 (M - H)⁻ (calcd for Chemical Formula: C₂₃H₂₀N₂O₇S⁻: 467.0918).

4.3.19 4-(piperidin-1-yl)-N-(1,2,8-trihydroxy-9-oxo-9H-xanthen-3-yl)benzenesulfonamide (**12s**)

Yield: 35%. ¹H NMR (400 MHz, DMSO-*d*₆) δ 11.77 (s, 1H), 11.57 (s, 1H), 9.92 (s, 1H), 9.63 (s, 1H), 7.76 – 7.66 (m, 3H), 7.07 – 6.94 (m, 4H), 6.78 (d, *J* = 8.2 Hz, 1H), 3.32 (s, 4H), 1.54 (s, 6H). ¹³C NMR (151 MHz, DMSO) δ 184.10, 160.05, 155.70, 153.39, 148.81, 146.68, 137.30, 135.89, 129.35, 128.55, 125.46, 113.10, 110.10, 107.17, 106.85, 103.16, 94.98, 47.44, 24.69, 23.70. MS (ESI) *m/z* 480.9 (M - H)⁻. HRMS (ESI) *m/z*: 481.1070 (M - H)⁻ (calcd for Chemical Formula: C₂₄H₂₂N₂O₇S⁻: 481.1075).

4.4 General biological evaluation procedures

4.4.1 In vitro PGAM1 enzyme inhibitory activity assay

1 μL of test compound (dissolved in DMSO) with specific concentration, 1 μL of recombinant PGAM1 and 48 μL of Tris buffer solution (50 mM, pH 8.0) were added into a 96-well plate followed by preincubated for 2 min at room temperature. Then 49 μL of enzymes buffer (containing 0.5 U/mL enolase, 0.5 U/mL PK, 0.1 U/mL LDH, 5 mM MgCl₂, 1 mM ADP, 100 mM KCl, 0.2 mM NADH, 100 mM Tris pH8.0) was added to the mixture. At last, 1 μL of 3PG solution (200 mM) was added to initiate the reaction. The decrease in OD (λ=340 nm) from the oxidation of NADH was measured by a microplate reader as PGAM1 activity.

Counterscreen assay: 1 μL of test compound (0.5 mM) and 49 μL of Tris buffer solution (50 mM, pH 8.0) were added into a 96-well plate followed by preincubated for 2 min at room temperature. Then 49 μL of enzymes buffer (containing 0.5 U/mL enolase, 0.5 U/mL PK, 0.1 U/mL LDH, 5 mM MgCl₂, 1 mM ADP, 100 mM KCl, 0.2 mM NADH, 100 mM Tris pH8.0) was added to the mixture. At last, 1 μL of 2PG solution (200 mM) was added to initiate the reaction. The decrease in OD (λ=340 nm) from the oxidation of NADH was measured as counter-screen assay activity.

4.4.2 Thermal shift assay of **12q**

In brief, thermal shift assay of **12q** with PGAM1 was performed in 384-well PCR plates with different concentrations of **12q** (from 12.5 μM to 50 μM) and 200 μg/ml protein in a buffer solution (20 mM Tris-HCl, 100 mM NaCl, pH 7.4). SYPRO orange was used as a dye to monitor the fluorescence change at 610 nm.

4.4.3 In vitro cell proliferation inhibitory activity assay

Cell viability was measured using MTT colorimetric assay. 2×10³ cells were seeded in 96-well plate before the assay starts and were cultured at 37 °C. After seeding for 24 h, cells were treated with inhibitors with specific concentration and incubated at 37 °C for 72 h followed by incubation with 0.5 mg mL⁻¹ MTT for 4 h at 37 °C. 200 μL of DMSO was added and absorbance was measured at 570 nm.

Acknowledgements:

This work was supported by the National Natural Science Foundation of China (No 21472026 to Lu Zhou), the Shanghai Municipal Committee of Science and Technology (No 14XD1400300) and the program for Shanghai Rising Star (No 15QA1400300).

References:

- [1] R.A. Cairns, I.S. Harris, T.W. Mak, *Nature Reviews Cancer*, 2011; 11: 85-95.
- [2] D. Hanahan, R.A. Weinberg, *Cell*, 2011; 144: 646-674.
- [3] J.R. Cantor, D.M. Sabatini, *Cancer Discovery*, 2012; 2: 881-898.
- [4] M.G. Vander Heiden, L.C. Cantley, C.B. Thompson, *Science*, 2009; 324: 1029-1033.
- [5] C. Zhao, L. Weiqin, G.-P. Celia, et al., *J Bioenerg Biomembr*, 2007; 39: 267-274.
- [6] M.G. Heiden, *Nature Reviews Drug Discovery*, 2011; 10: 671-684.

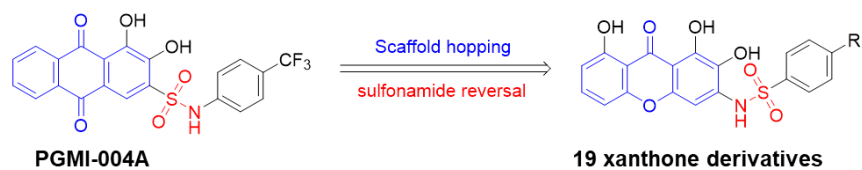
- [7] F. Ori, J. Livnat, F. Christian, et al., *Mol Syst Biol*, 2011; 7: 501.
- [8] C. Heesun, L. Chao, L. Tullia, et al., *Nat Biotechnol*, 2012; 30: 671-678.
- [9] J. Miran, S.K. Sung, L. Jinhwa, *Exp Mol Med*, 2013; 45: e45.
- [10] U.E. Martinez-Outschoorn, M. Peiris-Pages, R.G. Pestell, et al., *Nat Rev Clin Oncol*, 2017; 14: 11-31.
- [11] A.B. Walter, R.K. Jeremy, *Biochemistry*, 1980; 19: 738-743.
- [12] L.A. Fothergill-Gilmore, H.C. Watson, *Adv Enzymol Relat Areas Mol Biol*, 1989; 62: 227-313.
- [13] S. Sakoda, S. Shanske, S. DiMauro, et al., *J Biol Chem*, 1988; 263: 16899-16905.
- [14] N. Durany, J. Joseph, O.M. Jimenez, et al., *Br J Cancer*, 2000; 82: 20-27.
- [15] N.K. Narayanan, B.A. Narayanan, D.W. Nixon, *Cancer Detect Prev*, 2004; 28: 443-452.
- [16] C. Li, Z. Xiao, Z. Chen, et al., *Proteomics*, 2006; 6: 547-558.
- [17] D. Turhani, K. Krapfenbauer, D. Thurnher, et al., *Electrophoresis*, 2006; 27: 1417-1423.
- [18] R. Fenglian, W. Hong, L. Yunlong, et al., *Mol Cancer*, 2010; 9: 1-17.
- [19] X.C. Peng, F.M. Gong, Y. Chen, et al., *J Proteomics*, 2016; 132: 85-92.
- [20] M.J. Evans, A. Saghatelian, E.J. Sorensen, et al., *Nat Biotechnol*, 2005; 23: 1303-1307.
- [21] H. Taro, Z. Lu, E. Shannon, et al., *Cancer Cell*, 2012; 22: 585-600.
- [22] L. Xiaoguang, T. Shuai, W. Qian-Qian, et al., *Front Pharmacol*, 2017; 8: 325.
- [23] Q. Jia, S. Wenyi, Z. Jie, et al., *J Cell Biol*, 2017; 216: 409-424.
- [24] D. Zhang, N. Jin, W. Sun, et al., *Oncogene*, 2016; 36: 2900-2909.
- [25] D. Zhang, H. Wu, X. Zhang, et al., *J Cancer*, 2017; 8: 1943-1951.
- [26] H. Taro, Z. Lu, F. Jun, et al., *Nat Commun*, 2013; 4: 1790.
- [27] C. Barbara, G. Eyal, *Cancer Cell*, 2012; 22: 565-566.
- [28] M.J. Evans, G.M. Morris, J. Wu, et al., *Mol Biosyst*, 2007; 3: 495-506.
- [29] N. Khan, F. Afaq, M. Saleem, et al., *Cancer Res*, 2006; 66: 2500-2505.
- [30] P. Alja, V. Marjan, D. Marija Sollner, *Archives of Industrial Hygiene and Toxicology*, 2016; 67: 169-182.
- [31] S. Gil, P. Palanca, V. Sanz, et al., *J Nat Prod*, 1990; 53: 1198-1211.
- [32] J.P. Wolfe, J. Ahman, J.P. Sadighi, et al., *Tetrahedron Lett*, 1997; 38: 6367-6370.

Highlights

- A series of xanthone derivatives were discovered as novel phosphoglycerate mutase 1 inhibitors.
- **12q** with IC_{50} of 0.5 μ M, was the most effective PGAM1 specific inhibitor so far
- **12r** could effectively inhibit H1299 cell proliferation at micromolar level

ACCEPTED MANUSCRIPT

Graphical abstract



PGMI-004A

19 xanthone derivatives

PGAM1: IC₅₀ = 13.1 μMH1299: IC₅₀ = 25.6 μM**12q** R = cyclohexyl, PGAM1: IC₅₀ = 0.5 μM, H1299: IC₅₀ = 10 μM**12r** R = pyrrolidin-1-yl, PGAM1: IC₅₀ = 2.7 μM, H1299: IC₅₀ = 5 μM

Discovery of xanthone derivatives as novel phosphoglycerate mutase 1 inhibitors.